

*A technique of using coherent vortex formations of the dead-end zone of the vortex chamber of the end type as a controlling factor influencing the structure and characteristics of the output flow has been developed. The kinematic parameters of the flow relative to chambers with elongated and extremely short dead-end parts in the range of Reynolds numbers according to the parameters of the nozzle  $Re=47080-86530$  were investigated. The reaction of the flow structure in the output sections of the vortex chambers was determined experimentally using thermoanemometry. Profiles of time-averaged transversal and axial velocity projections, as well as corresponding values of the relative intensity of velocity pulsations, were obtained. It was found that at  $Re=86530$ , the elongation of the dead-end part of the chamber leads to a decrease in the initial cross-section of the transversal component by 15 % with an increase in the axial component by 19.7 %, and, at  $Re=47080$ , to a decrease in the transversal component by 21 % with an increase in the axial component by 8.5 %. This indicates the redistribution of kinetic energy from transversal to axial energy motion, which is confirmed by the analysis of the corresponding intensity profiles of the velocity pulsations in the output section of the chamber in the near-wall and near-axis zones of the flow. The integral intensity of the velocity pulsations along the initial cross-section of comparable chamber designs increases in a chamber with an elongated dead-end part with almost no additional energy losses. The obtained results form the basis of a rational method of controlling the macro- and microstructure of flows, which determines the efficiency of mass exchange and heat exchange processes in vortex chambers of the end type. Such designs are characteristic of vortex mixers, burners of industrial furnaces, furnace devices of hot water and steam boilers, and other technological and power equipment*

**Keywords:** *vortex chamber, thermoanemometer, control, vortex structure, speed profile, pulsation intensity*

# DEVELOPMENT OF AN UNTRADITIONAL TECHNIQUE TO CONTROL THE STRUCTURE OF THE OUTPUT FLOW FROM A VORTEX CHAMBER

**Volodymyr Turyk**

*Corresponding author*

PhD, Associate Professor

Department of Applied Fluid Mechanics and Mechatronics

National Technical University of Ukraine «Igor Sikorsky

Kyiv Polytechnic Institute»

Peremohy ave., 37, Kyiv, Ukraine, 03056

E-mail: turick46@gmail.com

**Viktor Kochin**

PhD, Senior Researcher\*

**Volodymyr Moroz**

PhD, Senior Researcher\*

**Dmytro Miliukov**

Head Technologist

JSC «MERIDIAN» named after S. P. Korolyov

Vatslava Havela blvd., 8, Kyiv, Ukraine, 03124

\*Research Department of the Information Systems

in Hydroaeromechanics and Ecology

Institute of Hydromechanics of NAS of Ukraine

Maria Kapnist str., 8/4, Kyiv, Ukraine, 03680

Received date 14.09.2022

Accepted date 22.11.2022

Published date 30.12.2022

**How to Cite:** Turyk, V., Kochin, V., Moroz, V., Miliukov, D. (2022). Development of an untraditional technique to control the structure of the output flow from a vortex chamber. *Eastern-European Journal of Enterprise Technologies*, 6 (8 (120)), 55–64.

doi: <https://doi.org/10.15587/1729-4061.2022.268516>

## 1. Introduction

The efficiency of hydrodynamic and heat exchangers used in energy, aircraft and shipbuilding, chemical technologies, etc. is largely determined by the characteristics of vortex formations and their interaction. Nevertheless, the theory of vortex systems is still far from complete due to the extraordinary complexity of nonlinear processes of origin, development, and interaction of vortex structures, especially in turbulent flows [1]. The same applies to insufficiently studied processes of formation of coherent vortex structures (CVS) in vortex chambers (VC). The fields of centrifugal forces in the VC cavities create radial and axial pressure gradients, which, together with the effects of instability of the boundary layers near the curvilinear walls of the chambers, significantly complicates the structure of shear currents [2]. In practice, the impossibility of unambiguous prediction of flow parameters significantly increases the time and labor costs while refining

experimental VC samples without guarantees of choosing the most rational structures.

Typical for studies of VC aerodynamics in most countries (USA, Germany, Great Britain, etc.) is the traditional attention to devices in which the main axial flow is given tangential motion by coaxial front devices in the form of axial-scapular, axial-tangential, auger, tangential-slit twist-ers [2]. Such devices can be called direct-flow devices since they do not have dead-end parts with a blind end. Their designs are typical of combustion chambers of gas turbine engines, some furnace burners of industrial furnaces, etc.

In studies of VC flows of the end type, that is, with a one-sided arrangement of the blind end relative to the nozzle assembly, attention was paid to the characteristics of the flow only in the flow («active») parts of the chambers at the macro level – pressure losses, friction coefficients, average heat transfer [3]. The only exception was the long-standing detection of the so-called «end effect» in the shortest possible

vortex valve chamber [4]. It involved the inexplicable ingress of the share of the stream from the region of the nucleus in the middle zone of the chamber to the end disc, followed by the formation in its boundary layer of spiral trajectories of motion of liquid particles directed to the center. The root cause of this effect, as well as the influence of the depth of the location of the blind end on the characteristics of the twisted flow at the outlet of the VC, have not been investigated.

However, dead-end flow regions exist in the piston zones of cylinders of two-stroke diesel engines, in many technological and energy systems of the end type. The length of such parts may be different depending on the specific design schemes of the devices. The dead-end parts of the VC form zones that have often been called «dead» because of the traditional idea of the random, unstable, and even «stagnant» nature of the current in them. Usually, in the practice of designing systems, such zones (subject to their technological need) had to be reduced as much as possible. First, it is caused by the widespread opinion about the uselessness of the complication and the impossibility of taking into account the aerohydrodynamic process in devices by adding the stagnant, irregular nature of the flow in their dead-end zones. It was believed that the interference of the vortex structures of these zones and the main flows can lead to a deterioration in the characteristics of the created devices (primarily due to the danger of increasing energy losses during the workflow). Secondly, the reduction of dead-end parts of devices is caused by a natural desire to prevent the deterioration of their mass-dimensional indicators. Therefore, general pictures of the flow in dead-end zones, and even more so a thorough study of their structure and influence on the initial parameters of flows, as a rule, did not arouse the interest of researchers. However, the development of «subtle» methods for controlling the structure of flows to increase the efficiency of the workflows of vortex devices, in particular the end type, should provide the most complete picture of the physical pattern of limited twisted turbulent currents. After all, it is known that during the formation of CVS by synchronization of their frequencies, energy can be distributed not throughout the entire spectrum of mods but selectively [5]. In the case of VC, this effect of the susceptibility of vortex formations in the interaction of flows of dead-end and flow parts can lead to a resonant or anti-resonance response in the characteristics of the output flow [6]. Non-clarified features of the process in any elements of the VC structures contain either a source of negative anomaly or a reserve for optimizing the processes of heat and mass transfer, mixing or separation of working media, as well as reducing the hydraulic resistance of vortex devices.

It was precisely because of the insufficient knowledge of the influence of the CVS of the dead-end parts of the VC of the end type on the characteristics of the output flow that there were no attempts to use these CVS for directional control of these characteristics. This control technique is not traditional, so there is reason to consider experimental research aimed at testing it relevant.

---

## 2. Literature review and problem statement

---

Known works on the problems of hydrodynamics of vortex and twisted flows can be divided into two main groups. The first, quite fully represented by monograph [1] with a wide bibliography on this problem, reflects the study of the types and features of specific vortices regardless of specific types of devices. Such works have a certain general theoretical signi-

ficance for the creation of a fundamental theory of the interaction of vortex systems, which has not yet received its final development. The second, more numerous group considers macrostructural engineering approaches to the analysis of currents in industrial vortex devices [2, 3]. This applies to studies, as a rule, of integral patterns of flow using thermo- and laser anemometry, PIV-methods, and powerful CFD software [7]. Such typical approaches to solving problems of this direction dominated. In [8], they analyzed the characteristics of the twisted flow in the VC of a flat vortex valve of the rocket engine thrust control system. The length of the chamber is much shorter than its diameter. Firstly, such a geometric feature is not typical for VC for energy or chemical-technological purposes. Secondly, according to the constructed PIV-vector velocity diagrams in one cross section of the valve, as well as by rather chaotic current lines according to Fluent CFD analysis, it is difficult to judge the microstructure of the flow, especially in a very important wall area. In [9], the author studied the influence of the diameter of the device of the so-called vortex gripper on the effect of suction. The author's main attention was focused on creating a twisted air flow of vacuum in the capture device. A simplified theoretical model of the flow field and a rough estimate of the distribution of the circular velocity according to these pressure measurements only revealed high-speed rotating flow in the inner wall of the VC and low-speed flow in the central part of the chamber. At the same time, the author admits that the theoretical forecast of the velocity distribution turned out to be shifted relative to the real one. There are known attempts at numerical modeling of the flow based on the averaged Navier-Stokes equations (RANS) in the VC of jet vortex chamber pumps. Thus, the results of the study helped to optimize the geometric and averaged operating parameters of the vortex chamber pump in work [10] and to propose a model of fluid boiling in the input section of the VC, taking into account the influence of an oblique cut of the active nozzle in [11]. These are certainly useful results in the sense of a clearly defined engineering direction since they do not go beyond the utilitarian goals set by the authors. This feature can be fully attributed to a similar research methodology, for example, in works on bidirectional VC [12, 13] and other works of this widespread direction.

Typical for the CFD ANSYS package, multi-colored flow patterns in accordance with the average velocity distribution more schematically reflect a large-scale picture of flows in the VC than give a detailed idea of the fine structure of the flow. This feature is a fundamental problem when expanding the range of problems of the turbulent flow in the direction of finding new methods of low-cost control of the characteristics of flows. By definition, it is not combined with the concept of mutual susceptibility of vortex structures [14], which is developed in [6] and undoubtedly has a perspective on the studied class of currents in the fields of mass forces [15].

It is known that the positive result of modeling by specialized software of complex hydro-aerodynamic processes is determined mainly by the successful selection of an artificial turbulent model and the technology of its application in accordance with the design features of the device [7]. The forced element of heuristics of such a solution to the problem is due to the lack of strict mathematical conditionality of the Navier-Stokes and Reynolds equations [16], on which almost all versions of universal CFD software products are built. There is also a fundamental physical problem that has not been solved so far. In shear turbulent currents, the central boundary theorem of Lyapunov is not fulfilled with respect to the set of

vortices that form the actual structure and characteristics of the flow. At the same time, there are deterministic connections between the components of the turbulent flow, which lead to the formation and interaction of CVS of different scales [14]. This dualism of the nature of turbulence in flows leads to the mathematical uncertainty of the mechanism of impulse transmission [16]. Therefore, universal programs for the correct theoretical and numerical description of real pictures of turbulent motion with the reproduction of the microstructure of the flow, in particular in the cavities of the VC, do not yet exist.

In the historical aspect, it is necessary to note the attempts of purely mathematical modeling of the flow in the dead-end zone of the chamber. This applies, for example, to the use of the classical method of conformal transformations to describe the process of blowing cylinders of internal combustion engines when the piston stops at dead points [17]. This method is based on the assumption of the potential of a two-dimensional flow of a non-viscous medium, which makes it under these conditions mathematically determined. But from the point of view of physics, the obtained results, by definition, cannot correctly reflect the complex three-dimensional structure of a viscous flow, especially taking into account the action of centrifugal effects and the loss of stability of movement near curvilinear walls. The experience of such modeling can be assessed positively in the context of the development of some applied applications of the theory of functions of a complex variable or only as the first approximation at the stages of a schematic representation of the processes under study.

In reality, the practice of creating vortex devices is based on previous experience of their design and hypothetical ideas about the flow in them. Then, at the stage of finishing the prototype, certain constructive improvements are made as a means of optimizing the control effects on the integral hydro- or aerodynamic characteristics of the device.

In experimental work [14], an explanation of the «end effect» was given and it was shown that the emergence of the radial component of the rotating motion of the gas mass at the end in the direction of its center is only one of the manifestations of the generalized flow pattern. At the macro and micro levels, the presence of fully ordered and mutually agreed CVS in the dead-end part of the VC was revealed. The conditions of formation and evolution of these CVS during certain transformations of the semi-limited input jet to VC, as well as under the influence of centrifugal instability of the flow near the curvilinear walls, are analyzed. This opens the prospect of creating a new direction of improving the efficiency of VC workflows – the direction of applying «subtle» influences on the structure of flows at the stage of their formation [6]. Such control ac-

tions can be carried out with the help of CVS both organically present in the vortex device [14] and artificially created [15]. After all, it is the CVS and, in particular, their low-frequency components, that most affect turbulent diffusion, processes of transfer of mass, momentum and energy in flows [5].

Thus, there is a fundamental possibility of controlling the characteristics of the flow in vortex devices using the depth factor of the dead-end zone that generates the CVS. However, the reaction of the structure of the twisted output flow of the chamber to the CVS of the dead-end zone when its depth changes is not sufficiently investigated. The great complexity of the processes of formation, evolution, and interaction of CVS makes it very difficult to describe them. Thus, the construction of the theory of «subtle» influences on the structure of the initial flows of VC in order to improve their characteristics requires a detailed study of the mechanisms of these influences by staging many experimental studies. This is the motivation for this work.

### 3. The aim and objectives of the study

The purpose of the work is to develop an unconventional way to control the initial characteristics of the flow in the VC formed by the CVS in its elongated dead-end part. This will make it possible to intensify the processes of mixing the medium, and therefore, mass and heat transfer, without significant energy losses in the technological and energy equipment of the vortex principle of operation.

To accomplish the aim, the following tasks have been set:

- to establish the peculiarities of the influence of the CVS of the dead-end zone of the VC on the nature of the profiles of the components of the average speed in the gas flow at the outlet of the chamber;
- to determine the reaction of the intensity of pulsations of the velocity by magnitude and spatial distribution in the initial cross-section of the chamber on the CVS in its elongated dead-end part.

### 4. Materials and research methods

#### 4.1. Equipment used in the experiment

The object of our study is the controlling action of the coherent structures of the vortex chamber on the initial characteristics of the gas flow to improve the mixing processes in it. The study was carried out on an experimental aerodynamic installation, schematically shown in Fig. 1.

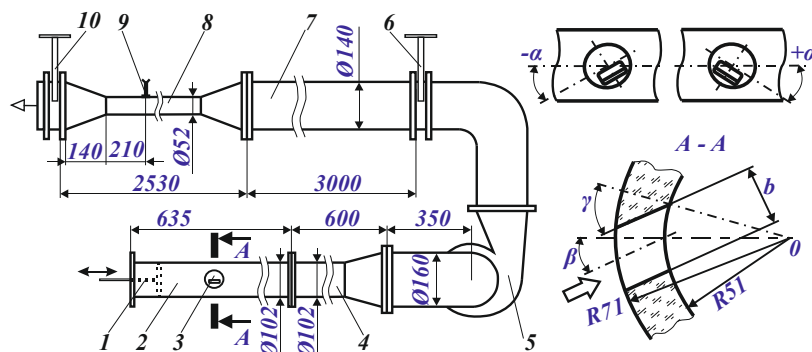


Fig. 1. Experimental installation: 1 – movable blind end; 2 – vortex chamber; 3 – entrance nozzle; 4 – intermediate damping insert; 5 – centrifugal fan; 6, 10 – gates; 7 – stabilization section; 8 – measuring section; 9 – flow-measuring pneumometric tube of «pencil» type

The working area was a vortex chamber of the end type with an internal diameter  $d_0=0.102$  m, which is made of organic glass to be able to visualize a complex flow in its cavity and to control the installation of the sensor. The flow part of the nozzle with a cross section measuring  $0.041 \times 0.025$  m<sup>2</sup> provided an angular orientation of the input flow  $\gamma=88^\circ$ ;  $\alpha=0^\circ$  in the range of Reynolds numbers according to the parameters of the nozzle  $Re=47080 \div 86530$ . The reaction of the structure of the output flow to the change in the relative depth of the dead-end zone VC  $L^*=L/d_0$  (where  $L$  is the distance from the inner edge of the initial cross-section of the nozzle to the blind end) was investigated at two limit values  $L^*=0$  and 4.4.

**4. 2. Procedure of measuring the speed and intensity of speed pulsations**

The program of the study involved instrumental measurement of actual values of air velocity in the output section of the VC along its vertical diameter. For this purpose, thermal anemometry equipment of constant temperature DISA-55 M (firm «DISA Elektronik», Denmark) with wire sensors was used. The equipment includes the bridge 55M10 (a bridge ratio of impedances of passive and active arms 1:20, upper frequency limit 200 kHz), power supply 55M01, digital voltmeter of average values 55D31, voltmeter of RMS values 55D35. The sensing elements of the sensors were platinum threads with a diameter of 5 μm and a length of  $10^{-3}$  m. The maximum systematic errors of the measuring system were as follows: relative to the orientation of the sensor sensing element with respect to the flow – 2.0 %; for the bridge 55M10, 0.21 %; for the digital voltmeter 55D31 – 2.0 %. The measurement zone of actual velocities was located at a distance of  $4.18 d_0$  from the center of the input nozzle (Fig. 2).

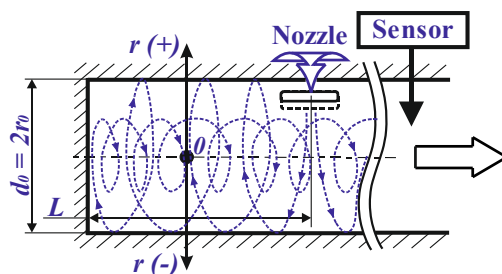


Fig. 2. Schematic of the vortex chamber and measurement area

Signals from the wired sensor were sent to the thermal anemometer devices and to the computer. The bridge of thermoanemometric equipment through the Butterworth low-frequency filter was connected to a 12-bit analog-to-digital converter (ADC) L-264 from L-Card with a systematic measurement error of 0.2 %. ADC is installed as an expansion board to the IBM-compatible computer UNO-3074-C11E (Advantech Co., Ltd., Taiwan) for recording and processing experimental data.

Based on preliminary measurements of the operating frequency range corresponding to the action of vortex systems in the dead-end and flow parts of the VC, the frequency of polling information from one sensor, taking into account the condition of the Kotelnikov theorem, was  $f=500$  Hz. The implementation time of one sample was 100 seconds, so each implementation provided for  $500 \times 100 = 50,000$  measurements. The conversion of the analog form of signals into digital allowed the application of the technique of statistical processing of time series (samples) of primary research data based on the

licensed software package «PowerGraph Professional» and built-in functions of Excel (Microsoft Corporation, USA).

As a result, the following statistical parameters were highlighted: time-averaged local axial  $W$  and transversal  $U$  velocity components; corresponding standard values of velocity pulsations  $\sqrt{\overline{w}^2}$  and  $\sqrt{\overline{u}^2}$  (standard deviations); relative intensity of pulsations at different points of the original cross-section of the VC. These components of speed are chosen due to the fact that their values significantly dominate the values of the radial component of the twisted flow velocity in the output cross section of the chamber.

For a constant temperature thermoanemometer according to the generally accepted procedure [18], there is a relationship between the voltage drop  $E$  in the diagonal of the bridge and the time-averaged component  $V_i$  of the local flow rate in the form:

$$E^2 = E_0^2 + B \cdot V_i^n,$$

where the exponent  $n$  is selected in such a way that in the coordinates  $E^2 = f(V_i^n)$  of the calibration characteristic of the sensor, the experimental points are approximated in a straight line;  $E_0^2$  – fictitious value of the voltage square, obtained by extrapolating the calibration characteristic to the value  $V_i=0$ ; coefficient  $B = \tan^2 \theta$  – the angle of inclination of the straight calibration characteristic to the abscissa axis.

Hence, the value of the average speed can be calculated by the formula:

$$V_i = \left[ (E^2 - E_0^2) / B \right]^{1/n}.$$

According to [18], the relative intensity of the velocity pulsations (generally for any components of the velocity  $V_i$  and the corresponding velocity pulsations  $v_i'$ ) is found by the formula:

$$\frac{\sqrt{\overline{v_i'^2}}}{V_i} = \frac{2E}{n(E^2 - E_0^2)} \cdot e,$$

where  $e = \sqrt{e_{rms}^2 - e_{noise}^2}$ ;  $e_{rms}$  is the value of the measured value of the RMS voltage pulsation;  $e_{noise}$  – the value of the «noise» of the system, determined by the «cap» method.

The measurement error of the profiles of the average speed and RMS pulsations was no more than 5 %. Most of the error is due to the systematic component during the calibration of the thermoanemometer in the specialized wind tunnel «DISA Elektronik». The random component, reflected by the relative RMS error, was 0.12 % with a confidence probability  $P=0.90$ .

**4. 3. Physical prerequisites for determining the reaction of the output flow to control actions**

The physical prerequisites for the reaction of the flow to these control actions are due to the peculiarities of the formation of a shear flow in the VC of the studied type. In [14], the formation in the dead-end part of the VC of fully ordered large-scale CVS was revealed, four of which are the most significant. Fig. 3 shows the structure of axial motion of air along the axis  $x$  of the dead-end part of the VC in the form of isotes of dimensionless axial velocity  $W^* = W/W_a$  ( $W$  – average speed according to the original cross-section of the VC) depending on the dimensionless radius of the chamber  $r^* = r/r_0$ . Directly in the nozzle region of the VC, pairs of vortices are formed in the angular zones of the inlet nozzle and divergent

vortices of the Görtler-Ludwig type on the concave wall of the cylindrical surface of the chamber. Next, quasi-Taylor vortices are formed, absorbed by spiral energy-intensive coherent structures (ECVS) of the maximum angular moment 1. The latter diverge into dead-end and flowing («active») parts of the chamber. In the direction of the end the meandering annular vortex 2 moves. But the peripheral region of the current 3, as well as the central quasi-solid-state tornado-shaped vortex (CQTV) 4, formed near the blind end according to the mechanism of the Bödevadt vortex [14], move in the direction of the active part of the VC.

Processing of experimental data given in [14] and others showed that the volumetric flow rate in spiral ECVS 1 and annular vortex 2 of the dead-end zone of the VC contains up to 75 % of the flow rate.

In general, the nature of the above pattern of isote distribution has common features similar to the corresponding patterns for VC with a different axial orientation of the flow intake in the above parameter ranges.

Therefore, in this study, in order to fundamentally test the influence of large-scale CVS of the dead-end zone, which are connected to the active part of the input flow, it was decided to limit the output characteristics of the VC to one value of the axial angle of the nozzle:  $\alpha=0$ . The active part of the input stream is called the one that directly from the nozzle goes directly to the flow part of the chamber. With a depth of the dead-end part approaching zero, the entire input flow becomes active. Consequently, the assessment of such an impact in the simplest means of static control of the structure of the output stream applied in this work is of some interest.

The choice of the position of the initial cross-section of the VC was based on a comparison of the geometry of the spiral part of the active flow with the technological capabilities of the experimental installation for arranging the measurement zone. The problem of determining the mechanism and detailed quantitative description of the interaction of the set of CVS of the dead-end zone and the active part of the input flow of the VC is very difficult both in experimental and theoretical-numerical formulations. But an integral assessment of the influence of this interaction on the kinematics of the twisted flow at the outlet of the chamber can be carried out on the basis of analysis of the distribution patterns of the dominant components of the averaged velocity of the output flow and the corresponding values of the intensity of the pulsations of the velocity.

### 5. Results of the study of the reaction of the output flow to the change in the depth of the location of the dead end of the vortex chamber

#### 5.1. Influence of coherent vortex structures of the dead-end zone of the chamber on the velocity profiles in the original cross-section

The results of measurements of kinematic parameters are represented in the form of plots of dimensionless values of transversal  $U^*=U/W_a$  (Fig. 4) and axial  $W^*=W/W_a$  (Fig. 5) time-averaged components of the actual velocity in the original cross-section of the VC. The profiles of the velocity constituents are given at the relative depths of the dead-end zone  $L^*=4.4$  and  $L^*=0$  in the Reynolds number range  $Re=47080+86530$ .

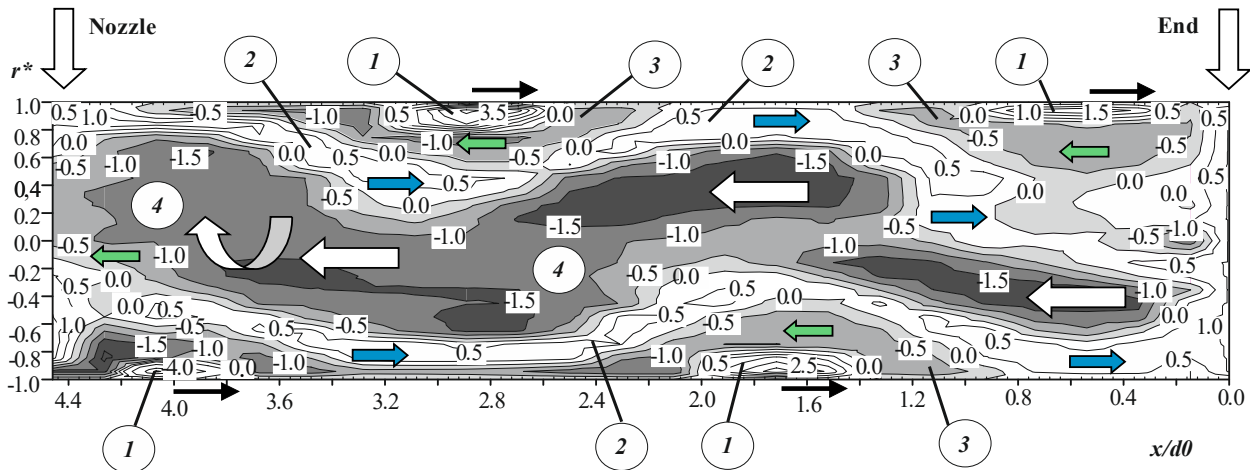


Fig. 3. An example of the distribution of isotes of dimensionless axial velocity in the dead-end part of the chamber at  $Re \approx 80000$ ;  $\gamma=88^\circ$ ;  $\alpha=0^\circ$  (white and light gray colors correspond to the direction of flow to the end; black and dark gray colors – from the end, with black corresponding to a higher speed) [14]

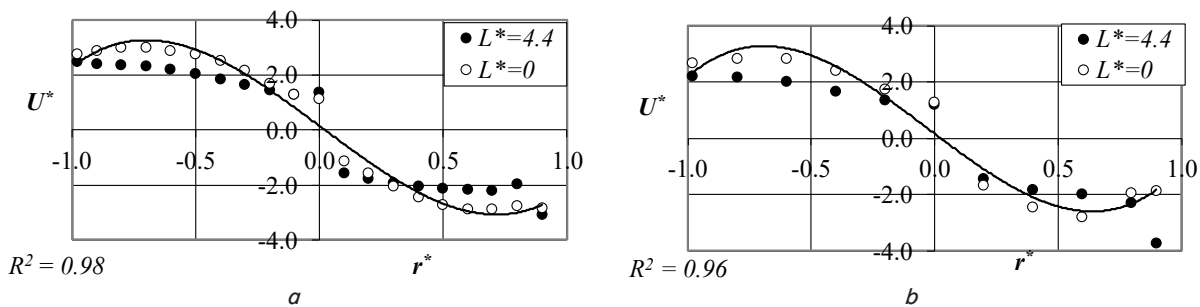


Fig. 4. Profiles of the transversal component of the average speed in the output section of the chamber:  $a - Re=86530$ ;  $b - Re=47080$

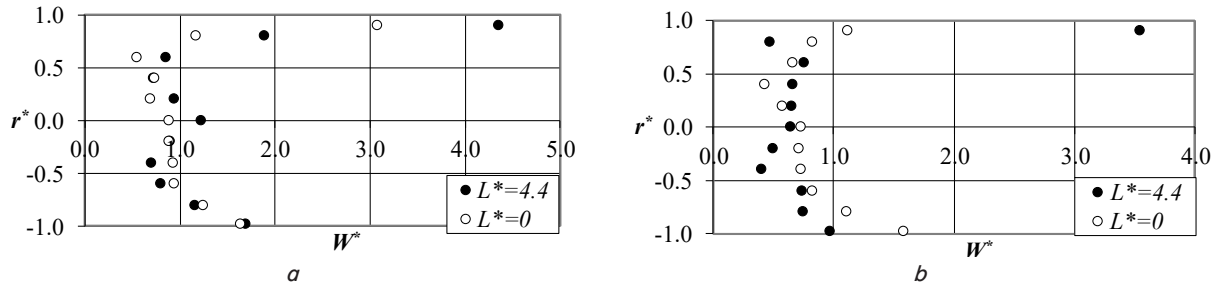


Fig. 5. Profiles of the axial component of the average speed in the output cross-section of the chamber: *a* – Re=86530; *b* – Re=47080

For clarity, in the case of  $L^*=0$ , the plots in Fig. 4 show the curves that approximate with the specified probability values  $R^2$  experimental points for the distribution of transversal velocity by polynomials of power 3. As can be seen from the plots, at  $L^*=4.4$ , in areas of dimensionless radius  $0.3 \leq |r^*| \leq 0.9$ , there is a decrease in the transversal velocity modulus compared to the case of  $L^*=0$  to 29 % at Re=86530 and to 30 % in areas  $0.4 \leq |r^*| \leq 0.8$  at Re=47080. Attention is drawn to the sharp increase in the transversal velocity modulus in the case of  $L^*=4.4$  at point  $r^*=0.9$  compared to point  $r^*=0.8$ : by 57 % at Re=86530 and by 62 % at Re=47080. This, at first glance, «anomaly» was confirmed by repeated repetition of the experiment.

As for the profiles of time-averaged axial velocities in the original cross-section of the VC, the following should be noted. As the plots show in Fig. 5, at Re=86530 in the range of dimensionless radii  $-0.9 \leq r^* \leq 0.9$ , the axial velocity distributions for the  $L^*=0$  and  $L^*=4.4$  variants are roughly similar with some asymmetry relative to the chamber axis. So, at Re=86530,  $L^*=4.4$ , in the range  $0 \leq r^* \leq 0.9$ , there is an excess of axial speed from 37 % to 62 %, but in the range of  $-0.8 \leq r^* \leq -0.4$  – a decrease in it from 7 % to 25 % compared to the chamber option  $L^*=0$ . In the case of  $L^*=4.4$ , at point  $r^*=0.9$ , compared to point  $r^*=0.8$ , an «anomaly» was again detected – a significant difference in the value of the axial velocity: up to 130 % at Re=86530 and up to 650 % at Re=47080. In addition, in the case of  $L^*=4.4$ , at radius  $r^*=0.9$ , at Re=47080 compared to the chamber variant  $L^*=0$ , there is an overspeeding of up to 217 % (against 42 % at Re=86530). In the radius range of  $0.2 \leq r^* \leq 0$ , at  $L^*=4.4$ , axial velocity is also exceeded compared to the  $L^*=0$  variant: from 38 % to 56 % at Re=86530, and from 13 % to 55 % at Re=47080. However, in the range of  $-0.98 \leq r^* \leq 0$  of the VC cross-section at Re=47080, there is a steady weakening of the axial velocity component for the chamber  $L^*=4.4$  compared to the  $L^*=0$  variant: from 30 % at  $r^*=-0.2$  to 45 % at  $r^*=-0.4$ , and up to 39 % at  $r^*=-0.98$ . Provided Re=86530, the attenuation is 15 % at  $r^*=-0.6$  and up to 25 % at  $r^*=-0.4$ . On the VC axis at Re=86530 and  $L^*=4.4$ , the axial velocity advantage of 39 % compared to the case of  $L^*=0$  is disturbed at Re=47080: the speed is 12 % less compared to the chamber of the parameter  $L^*=0$ .

**5. 2. The reaction of the intensity of the velocity pulsations in the output section of the chamber to the coherent structures of the elongated dead-end part**

Fig. 6 shows the distribution of the values of the relative intensity of the pulsations of the transversal  $\epsilon_u = \sqrt{u'^2}/U$  and axial  $\epsilon_w = \sqrt{w'^2}/W$  components of the velocity along the vertical diameter of the original cross-section of the VC.

The results of processing the measured values of the actual transversal velocity show the following. For chambers of variants  $L^*=4.4$  and  $L^*=0$  at the maximum and minimum va-

lues of the Reynolds Re number, the corresponding values of the relative intensity of pulsations increase to 300 % only in the radii range  $-0.5 \leq r^* \leq 0.5$  (Fig. 6, *a*). The specified nature of the distribution of the intensity of transversal pulsations of velocity, to some extent symmetrical with respect to the axis of the chamber, is not observed in the distribution of the intensity of axial pulsations (Fig. 6, *b*). In the latter case, at  $r^* > 0$ , there is a predominance of the intensity of axial pulsations compared to the zone  $r^* < 0$ .

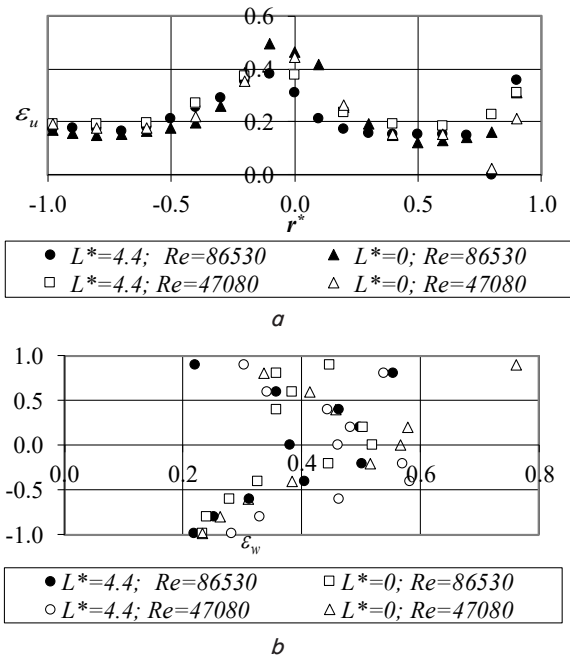


Fig. 6. Distribution of the intensity of pulsations in the output section of the chamber: *a* – transversal velocity; *b* – axial velocity

In general, the maximum intervals of the bulk of the experimental points of the profiles  $\epsilon_w(r^*)$  and  $\epsilon_u(r^*)$  are  $0.22 < \epsilon_w < 0.58$  (except for the radius  $r^*=0.9$ ) and  $0.12 < \epsilon_u < 0.5$  (except for the radius  $r^*=0.8$ ), respectively. Comparison of the diagrams of the values  $\epsilon_w(r^*)$  and  $\epsilon_u(r^*)$  in Fig. 6 shows that the greatest values of the intensity of pulsations of axial velocity occupy a much wider range of radii than the interval  $-0.5 \leq r^* \leq 0.5$  in the case of the distribution of transversal pulsations. For axial pulsations, the range boundaries practically coincide with the limits of the vertical chamber cross-section  $-0.98 < r^* < 0.9$ .

Comparative assessment of the redistribution of the intensity of pulsation motion for its various components is advisable to carry out thru the introduction of the parameter:

$$\delta\varepsilon = \frac{\bar{\varepsilon}_w - \bar{\varepsilon}_u}{\bar{\varepsilon}_u} \cdot 100\%, \tag{1}$$

where  $\bar{\varepsilon}_w, \bar{\varepsilon}_u$  – averaged by the selected zones the magnitude of the intensity of pulsations.

For a generalized estimate of the energy distribution of pulsation motion along the output section of the VC, we introduce the value of the relative integral intensity of the pulsations of the velocity:

$$\bar{\varepsilon} = \sqrt{\frac{1}{2}(\bar{u}'^2 + \bar{w}'^2)} / V_s, \tag{2}$$

where  $V_s = \sqrt{U^2 + W^2}$  is the local tangential velocity of a spiral twisted current at different points in the diameter of the original cross-section of the VC.

Fig. 7 shows the distribution of this parameter in the vertical output section of the chamber at  $Re=var$ .

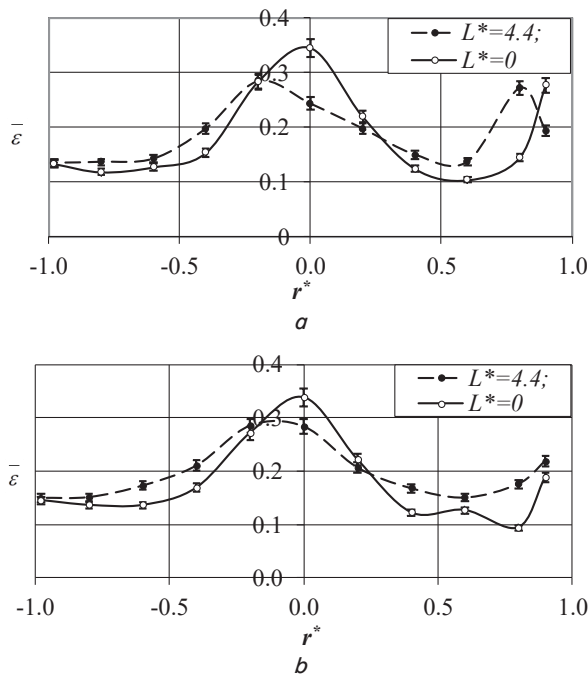


Fig. 7. Profiles of the relative integral intensity of velocity pulsations in the output section of the vortex chamber: *a* –  $Re=86530$ ; *b* –  $Re=47080$

On the plots in Fig. 7, authentic authors applied approximation by splines of experimental points indicating the confidence intervals of relative errors equal to 4.8 % (the maximum possible value) with a confidence probability of 0.9.

### 6. Discussion of results of the study of the influence of coherent structures of the dead-end part of the chamber on the structure of the output flow

An integral comparison of profiles of averaged transversal velocity components in the range of dimensionless radii  $r^* = -0.98 \div 0.9$  for both types of VC (Fig. 4) shows the following. There is not only an improvement to 30 % of the uniformity of profiles at the output of the chamber  $L^* = 4.4$  but also a decrease in the average transversal velocity by 15 % at  $Re=86530$  and by 21 % at  $Re=47080$  compared to chamber

variant  $L^* = 0$ . Consequently, the CVS of the dead-end part of the VC in a certain way streamline the structure of the output stream of the chamber. This reflects the effect of the principle of mutual susceptibility of vortex structures [6, 14, 15], which, in this case, are formed by the input flow to the VC. The peculiarity of their formation in the chamber satisfies the necessary conditions of this principle. They imply the consistency of the excitation axes of vortex systems, as well as in the obvious commensuration of their geometric and energy characteristics due to the interconnected flow topology in the dead-end and active zones of the chamber.

The regular nature of the distribution of research points at the limit values of the relative depth of the dead-end part of the VC indirectly indicates the falsity of traditional ideas about the so-called «dead zone» in the dead-end regions of the end-type chambers. The random nature of the disordered flow in the «dead zone» would have to appropriately affect the velocity profile in the original cross-section of the VC, which is not observed in the experiments.

A sharper increase in the transversal velocity modulus at  $L^* = 4.4$  at the point  $r^* = 0.9$  for  $Re=47080$  compared to mode  $Re=86530$  is explained by the ingress of the maximum angular momentum into this zone of the active part of the ECVS. This fact is caused by a weakening of the flow self-ejection from the side of the end to the exit from the VC [14] and, accordingly, a significant increase in the volumetric fraction of the twisted active parts of the ECVS with a minimum value of the Reynolds number. But here the question arises as to the reason for the 97 % reduction in the transversal velocity module at point  $r^* = 0.9$  in the complete absence of the ejection of the input flow, provided  $L^* = 0$  and  $Re=47080$  compared to the  $L^* = 4.4$  variant. The answer becomes obvious if we take into account the increase in the step of the spiral trajectory of the near-wall ECVS under the specified conditions and the corresponding displacement of the zone maximum angular torque relative to a fixed cross-section of measurements at the output of the VC.

Regarding the distributions of axial speed, as can be seen from Fig. 5, the qualitative nature of them in the original cross-section of the VC for the compared variants of the VC has a certain similarity in a rather rough approximation. But under both flow modes by the Reynolds number, especially with its minimum value, there is a significant violation of the approximate similarity of axial velocity profiles for the compared VC variants in the region of radii  $r^* = 0.8$  and  $0.9$ . This is due to the already known reason for the difference in the steps of the spiral trajectory of the near-wall ECVS relative to the measurement zone for variants of chambers with  $L^* = 0$  and  $L^* = 4.4$ . Fig. 5, *b* illustrates the persistent attenuation of the axial velocity component in the lower half of the vertical diameter  $-0.98 \leq r^* \leq 0$  since the bulk of the spiral active flow passes through the upper part of the original VC cross section.

A comparable integral estimate of the values of time-averaged axial velocity components in the full range of dimensionless radii  $r^* = -0.98 \div 0.9$  of the original VC cross-section shows the following. When the parameter of the dead-end region changes from  $L^* = 0$  to the maximum value of  $L^* = 4.4$ , the average axial velocity increases by 19.7 % at  $Re= 86530$  and 8.5 % at  $Re=47080$ . An increase in the average axial velocity at the above reduction of the transversal component at  $Re=var$  in the case of an elongated dead-end part of the VC indicates a redistribution of kinetic energy from transversal motion to axial. In the process of energy exchange between

the types of gas movement, some radial component of the speed is also involved. High-quality visualization of the flow with fine powder  $\text{Al}_2\text{O}_3$  suggested that the influence of the radial component on the structure of a fully formed twisted flow in the exit zone from the chamber is much smaller compared to the influence of the remaining components of the velocity.

Let us dwell on the comparison of the intensity values of axial and transversal pulsations of the velocity. To do this, we analyze the reason for the greater occupancy of the profile  $\varepsilon_w(r^*)$  compared to the profile  $\varepsilon_u(r^*)$  for chambers with parameters  $L^*=4.4$  and  $L^*=0$ . Comparison of these profiles in Fig. 6 shows that the greatest values of the intensity of pulsations of axial velocity occupy a much wider range of radii than the interval  $-0.5 \leq r^* \leq 0.5$  in the case of distribution of transversal pulsations. For axial pulsations, the corresponding limits of the radius range coincide with the limits of the vertical section of the chamber  $-0.98 < r^* < 0.9$ . The nature of the transversal velocity profiles in the radii range  $-0.5 < r^* < 0.5$  (Fig. 4) also indicates a weakened suppression of transversal pulsations by centrifugal forces in this zone. This corresponds to the «surge» of  $\varepsilon_u$  values in a sufficiently narrow near-axis range of radii (Fig. 6, a). Instead, a more uniform distribution of axial velocities over the output section of the chamber, even in a larger range of radii (Fig. 5), corresponds to a more uniform distribution of values  $\varepsilon_w$ . In addition, in the chamber with  $L^*=4.4$ , the influence of the rotational-translational axial structure CQTV from the side of the dead-end zone with a significant axial component of the speed is added to the axial component of the velocity. It is the interaction of these two flows that creates the conditions for the redistribution of kinetic energy from the transversal component of the movement to the axial one, which weakens the blocking effect of centrifugal force on the pulsation. Integrally, this is manifested in the predominance of axial components as averaged velocity and relative intensity of velocity pulsations over transversal components. A certain variation of experimental data  $\varepsilon_w(r^*)$  at radii  $r^*=0$ ,  $r^*=0.2$  and  $r^*=0.9$  at  $\text{Re}=\text{var}$  may indicate an unequal influence of the reverse flow zone (RFZ) [2] on the active output flow, differently formed at  $L^*=\text{var}$ . This causes a change in the position of the zone of maximum momentum in the flow relative to the sensor of the thermoanemometer. Emissions of  $\varepsilon_w$  values at radii  $r^*=-0.4$  and  $-0.6$  are explained by the lack of coaxiality of RFZ relative to the axis of the chamber during one-sided tangential air supply to its cavity through a single nozzle.

A more detailed explanation of these features of the flow in the active zone of the chamber requires the formulation of additional studies involving spectral analysis of pulsations in several cross sections of a certain vicinity of the original section studied in this paper.

For approximate quantitative estimates of the effect of redistribution of pulsation energy relative to the variants of VC with  $L^*=0$  and  $L^*=4.4$ , we shall analyze the experimental data on the plots of Fig. 6 for the most characteristic flow zones. The «wall zone» of the current, introduced on the basis of the theory of turbulent flows in pipes and Fig. 3, corresponds to a range of dimensionless radii of  $0.8 \leq |r^*| < 1.0$ . The «near-axial zone» of the current is the range  $-0.2 \leq r^* \leq 0.2$ . The values of the parameter  $\delta\varepsilon$ , according to formula (1), for the two variants of the VC are given below.

For the chamber option with  $L^*=0$ , we have:

a) within the near-wall zone  $\delta\varepsilon \approx 43\%$  at  $\text{Re}=86530$  and  $\delta\varepsilon \approx 254\%$  at  $\text{Re}=47080$ ;

b) in the near-axial zone  $\delta\varepsilon \approx 8\%$  at  $\text{Re}=86530$  and  $\delta\varepsilon \approx 29\%$  at  $\text{Re}=47080$ .

For the chamber option with  $L^*=4.4$ , we have:

a) within the near-wall zone  $\delta\varepsilon \approx 55\%$  at  $\text{Re}=86530$  and  $\delta\varepsilon \approx 72\%$  at  $\text{Re}=47080$ ;

b) in the near-axial zone  $\delta\varepsilon \approx 9\%$  at  $\text{Re}=86530$  and  $\delta\varepsilon \approx 24\%$  at  $\text{Re}=47080$ .

Thus, in both characteristic zones of the flow at the output of the VC, with the studied geometric and regime parameters, the irregularity  $\delta\varepsilon > 0$  is firmly observed, which indicates a significant predominance of the kinetic energy of axial pulsations over transversal ones.

Obviously, the analysis of the distribution by the original cross-section of the VC of the values introduced by formula (2) of the relative integral intensity of the pulsations of the velocity  $\bar{\varepsilon}$  is of practical interest. Sure. We notice that according to Fig. 7, the behavior of experimental points in the near-wall zone at  $r^*=0.8$  and  $0.9$  is fully correlated with the values of  $\varepsilon_w$  at these points at  $\text{Re}=86530$ , and at the radius  $r^*=0.8$  and at  $\text{Re}=47080$  (Fig. 6, b). This fact seems logical given the predominance in the near-wall zone of the flow of energy of axial pulsations compared to transversal ones due to a decrease in the decrease in the average value of the transversal component of the velocity towards the wall. In general, the plots in Fig. 7 indicate a more symmetrical distribution of the energy of pulsation motion relative to the axis of the chamber according to the output section of the VC with the parameter  $L^*=4.4$ . Calculations show the following. The transition to the elongated dead-end part of the VC ( $L^*=4.4$ ) causes the following increase in value relative to the variant  $L^*=0$ : at  $\text{Re}=86530$  by 3%; at  $\text{Re}=47080$ , more than 11%.

It is important to emphasize that the measurement of full pressure losses for chambers of both variants carried out during the experiments showed the practical invariance of the aerodynamic drag of the chamber with the most elongated dead-end zone compared to the VC variant at  $L^*=0$ . Thus, at  $\text{Re}=86530$ , there is an increase in losses by 2.8%, and, at  $\text{Re}=47080$ , reducing them by 1%. These values are commensurate with the errors in measuring pressure and volumetric air flow for chambers of both types, so the resulting changes in the resistance of the VC can be ignored.

Thus, the first experience of using the studied unconventional method of controlling the structure of the output flow by coherent vortex formations of the elongated dead-end part of the VC showed a certain tendency to improve the mixing processes in the chamber cavity. But he also revealed the need for further improvement of the proposed control technique. It involves finding a method for balancing the intensity levels of velocity pulsations by individual components. Obviously, this can be achieved by varying the values of both the relative depth of the dead-end zone of the VC and the axial angles of installation of the input nozzle in order to determine the most optimal combination of these parameters.

The main limitations of this seminal study are the impossibility of applying the results obtained when changing the angles of  $\alpha$  and  $\gamma$  for supplying the input flow, as well as when switching to the VC with a dispersed gas supply.

The disadvantages of the work include the following. At this stage of the study, the assumption of neglect of the radial component of the velocity in the initial cross-section of the VC was based only on the qualitative visualization of the flow. Therefore, it needs further instrumental verification with a quantitative comparative analysis of the components of speed.

---

## 7. Conclusions

---

1. Experimentally, it was found that the coherent vortex structures of the elongated dead-end part of the vortex mixing chamber can be used to directly control the profiles of the constituent local gas velocities at the outlet of the chamber. In a vortex chamber with an elongated dead-end part of the relative depth  $L^*=4.4$  in the range of Reynolds numbers  $Re=47080-86530$ , there is an improvement in the uniformity of the profile of transversal components up to 30 % compared to the chamber at  $L^*=0$ . A corresponding decrease in the value of the average cross-section of the transversal component of the speed from 15 % to 21 % with a commensurate increase in the axial component indicates a commensurate increase in the axial component redistribution of kinetic energy from transversal motion to axial. This weakens the mechanism of blocking the effect of centrifugal force on the pulsation of speed and the process of mixing the working medium.

2. In a vortex chamber with an elongated dead-end part, a positive, from the point of view of facilitating the mixing process, reaction of speed pulsation intensity profiles in the output section of the chamber to the vortex structures of the dead-end region was determined. The reaction indicates a significant predominance of the kinetic energy of axial pulsations over the transversal ones both in the near-wall (up to 72 % at  $Re=47080$  and up to 55 % at  $Re=86530$ ) and in the near-axial (up to 24 % at  $Re=47080$  and up to 9 % at  $Re=86530$ ) flow zones. The use of an elongated dead-end part of the chamber leads to a more symmetrical pulsation energy distribution chamber relative to the axis in the flow at the exit from the chamber. In addition, an increase in the integral intensity of velocity pulsations in the output section of the vortex chamber up to 11 % was revealed. The indicated reaction of the distribution of the intensity of the pulsations of the speed is due to the interaction of the

rotational-translational axial vortex structure of the dead-end zone of the chamber with the «active» part of the input flow, directly directed from the nozzle towards the exit from the chamber. The obtained research results can form the basis for the practical development of a new method of controlling the flow structure in end-type vortex chambers in energy and technological equipment in order to improve its efficiency.

---

### Conflict of interest

---

The authors declare that they have no conflict of interest in relation to this research, whether financial, personal, authorship or otherwise, that could affect the research and its results presented in this paper.

---

### Financing

---

The study was conducted without financial support.

---

### Data availability

---

All data are available in the main text of the manuscript.

---

### Acknowledgments

---

The authors express their sincere gratitude to Doctor of Technical Sciences, Professor V. Babenko, for his constant attention to conducting research in the context of the development of the concept of mutual susceptibility of coherent vortex structures formulated by him, and for a number of useful tips in staging the current research.

---

## References

1. Alekseenko, S. V., Kuybin, P. A., Okulov, V. L. (2005). *Vvedenie v teoriyu kontsentrirrovannykh vikhrey*. Moscow-Izhevsk: Institut komp'yuternykh issledovaniy, 504.
2. Khalatov, A. A., Avramenko, A. A., Shevchuk, I. V. (2000). *Teploobmen i gidrodinamika v polyakh tsentrobezhnykh massovykh sil*. Vol. 3. Kyiv: In-t tekhn. teplofiziki NAN Ukrainy, 474.
3. Khalatov, A. A., Romanov, V. V., Borisov, I. I., Dashevskiy, Yu. Ya., Severin, S. D. (2010). *Teploobmen i gidrodinamika v polyakh tsentrobezhnykh massovykh sil*. Vol. 9. Kyiv: In-t tekhn. teplofiziki NAN Ukrainy, 474.
4. Wormley, D. N. (1969). An Analytical Model for the Incompressible Flow in Short Vortex Chambers. *Journal of Basic Engineering*, 91 (2), 264–272. doi: <https://doi.org/10.1115/1.3571091>
5. Babenko, V. V., Chun, H. H., Li, I. (2013). Boundary layer flow over elastic surfaces. Butterworth-Heinemann. doi: <https://doi.org/10.1016/C2011-0-06221-X>
6. Babenko, V. (2021). *Experimental Hydrodynamics for Flow Around Bodies*. Academic Press. doi: <https://doi.org/10.1016/C2019-0-04933-3>
7. Ferziger, J. H., Perić, M., Street, R. L. (2020). *Computational methods for fluid dynamics*. Springer, 614.
8. Wei, X. G., Li, J., He, G. Q. (2018). Swirl Characteristics of Vortex Valve Variable-Thrust Solid Rocket Motor. *Journal of Applied Fluid Mechanics*, 11 (1), 205–215. doi: <https://doi.org/10.29252/jafm.11.01.27658>
9. Wang, C., Zhao, J., Li, X. (2019). Effect of chamber diameter of vortex gripper on maximum suction force and flow field. *Advances in Mechanical Engineering*, 11 (3), 168781401983740. doi: <https://doi.org/10.1177/1687814019837401>
10. Rogovyi, A., Korohodskiy, V., Khovanskyi, S., Hrechka, I., Medvediev, Y. (2021). Optimal design of vortex chamber pump. *Journal of Physics: Conference Series*, 1741 (1), 012018. doi: <https://doi.org/10.1088/1742-6596/1741/1/012018>
11. Merzliakov, I., Pavlenko, I., Ochowiak, M., Ivanov, V., Agarwal, P. (2022). Flow Modeling in a Vortex Chamber of a Liquid–Steam Jet Apparatus. *Processes*, 10 (5), 984. doi: <https://doi.org/10.3390/pr10050984>

12. Sharma, G., Majdalani, J. (2021). Effects of nozzle inlet size and curvature on the flow development in a bidirectional vortex chamber. *Physics of Fluids*, 33 (9), 093607. doi: <https://doi.org/10.1063/5.0066121>
13. Sharma, G., Majdalani, J. (2022). Effects of various inlet parameters on the computed flow development in a bidirectional vortex chamber. *Physics of Fluids*, 34 (4), 043607. doi: <https://doi.org/10.1063/5.0089443>
14. Babenko, V. V., Turick, V. N. (2008). Maket vikhrevykh struktur pri techenii potoka v vikhrevoy kamere. *Prykladna hidromekhanika*, 10 (82 (3)), 3–19.
15. Turick, V., Kochin, V., Kochina, M. (2018). Examining the technique to control the structure of current in vortex chambers by wing vortex generators. *Eastern-European Journal of Enterprise Technologies*, 1 (5 (91)), 28–38. doi: <https://doi.org/10.15587/1729-4061.2018.121962>
16. Marsden, Dzh. E., Chorin, A. (2004). *Matematicheskie osnovy mekhaniki zhidkosti*. Moscow-Izhevsk: NITS «Regulyarnaya i khao-ticheskaya dinamika», 204.
17. Chaplygin, S. A., Golubev, V. V. (1934). K teorii produvki tsilindrov dvigateley vnutrennego sgoraniya. *Trudy TsAGI*, 175, 3–46.
18. Dyban, E. P., Epik, E. Ya. (1985). *Teplomassoobmen i gidrodinamika turbulizirovannykh potokov*. Kyiv: Nauk. dumka, 296